Development 135, 0000-0000 (2008) doi:10.1242/dev.009910

Role of epithelial cell fibroblast growth factor receptor substrate 2α in prostate development, regeneration and tumorigenesis

Yongyou Zhang[1,*], Jue Zhang[1,*], Yongshun Lin[1], Yongsheng Lan[1], Chunhong Lin[1], Jim W. Xuan[2], Michael M. Shen[3], Wallace L. McKeehan[1], Norman M. Greenberg[4] and Fen Wang[1,†]

The fibroblast growth factor (FGF) regulates a broad spectrum of biological activities by activation of transmembrane FGF receptor (FGFR) tyrosine kinases and their coupled intracellular signaling pathways. FGF receptor substrate 2α (FRS2α) is an FGFR interactive adaptor protein that links multiple signaling pathways to the activated FGFR kinase. We previously showed that FGFR2 in the prostate epithelium is important for branching morphogenesis and for the acquisition of the androgen responsiveness. Here we show in mice that FRS2α is uniformly expressed in the epithelial cells of developing prostates, whereas it is expressed only in basal cells of the mature prostate epithelium. However, expression of FRS2α was apparent in luminal epithelial cells of regenerating prostates and prostate tumors. To investigate FRS2α function in the prostate, the *Frs2α* alleles were ablated specifically in the prostatic epithelial precursor cells during prostate development. Similar to the ablation of *Fgfr2*, ablation of *Frs2α* disrupted MAP kinase activation, impaired prostatic ductal branching morphogenesis and compromised cell proliferation. Unlike the *Fgfr2* ablation, disrupting *Frs2α* had no effect on the response of the prostate to androgens. More importantly, ablation of *Frs2α* inhibited prostatic tumorigenesis induced by oncogenic viral proteins. The results suggest that FRS2α-mediated signals in prostate epithelial cells promote branching morphogenesis and proliferation, and that aberrant activation of FRS2-linked pathways might promote tumorigenesis. Thus, the prostate-specific *Frs2α*^{cn} mice provide a useful animal model for scrutinizing the molecular mechanisms underlying prostatic development and tumorigenesis.

KEY WORDS: Adaptor proteins, Growth factors, Receptor tyrosine kinases, Prostate cancer, Mouse models

INTRODUCTION

Prostatic tumors are the most frequently diagnosed tumors in American males. Yet, the mechanisms underlying prostate tumor initiation, progression and escape from regulation by androgen are not well understood. Since many developmental events are recapitulated during tumorigenesis, understanding prostate development will aid comprehension of prostate tumorigenesis. Prostate development starts at embryonic day 17 (E17), when a group of urogenital epithelial cells in the hindgut endoderm grow out into the surrounding mesenchyme and form the anterior, ventral, dorsal and lateral prostate buds (Donjacour and Cunha, 1988; Sugimura et al., 1986). The prostatic buds then undergo extensive branching morphogenesis prior to puberty. At pubertal stages, the prostate rudiments grow rapidly; the ducts elongate from distal points and exhibit complex infolding of the intraductal mucosum. It has been shown that several growth factor families, including the fibroblast growth factor (FGF) family, play important roles in regulating prostate morphogenesis (Donjacour et al., 2003; Huang et al., 2005; Lin et al., 2007a; Thomson and Cunha, 1999).

[1]Center for Cancer and Stem Cell Biology, Institute of Biosciences and Technology, Texas A&M Health Science Center, 2121 W. Holcombe Blvd., Houston, TX 77030-3303, USA. [2]Department of Surgery, University of Western Ontario, London, ON, N6A 4G5, Canada. [3]Departments of Medicine, and Genetics and Development, Columbia University, College of Physicians and Surgeons, Herbert Irving Comprehensive Cancer Center, 1130 St. Nicholas Avenue, Room 217B, New York, NY 10032, USA. [4]Clinical Research Division, Fred Hutchinson Cancer Research Center, 1100 Fairview Avenue, Seattle, WA 98109-1024, USA.

*These authors contributed equally to this work
†Author for correspondence (e-mail: fwang@ibt.tmc.edu)

Accepted 24 November 2007

The FGF family consists of 22 gene products controlling a wide spectrum of cellular processes. The FGF elicits regulatory signals by activating FGF receptor (FGFR) transmembrane tyrosine kinases encoded in isoforms of four genes (McKeehan et al., 1998; Powers et al., 2000; Wang and McKeehan, 2003). In the prostate, members of the FGF and FGFR families are partitioned between the epithelial and mesenchymal compartments and underlie directionally specific and reciprocal communication between the two compartments. Ablation of the FGF signaling disrupts prostate development (Donjacour et al., 2003; Huang et al., 2005; Lin et al., 2007a). Aberrant FGF signaling, in particular the reduction in the resident epithelial FGFR2IIIb, the ectopic appearance of FGFR1, and the overexpression of FGF9 in epithelial cells, is associated with prostate tumor progression (Giri et al., 1999; Jin et al., 2003b; Kwabi-Addo et al., 2001; Lu et al., 1999; McKeehan et al., 1998; Polnaszek et al., 2004; Ropiquet et al., 1999).

Recently, we reported that ablation of FGFR2 in prostatic epithelial precursor cells in early prostate development inhibits prostatic ductal branching morphogenesis and the acquisition of androgen dependency during development (Lin et al., 2007a). Similarly, ablation of *Fgf10*, a ligand for the FGFR2IIIb isoform, also disrupts prostate development (Donjacour et al., 2003; Huang et al., 2005). The detailed mechanism underlying how FGFR2 elicits intracellular regulatory signals in the prostate remains elusive. FRS2α is an adaptor protein that links FGFR kinases to multiple downstream signaling pathways. Activation of the MAP kinase and phosphatidylinositol 3 (PI3) kinase pathways by FGFR1 is primarily mediated via FRS2α (Kouhara et al., 1997; Lin et al., 1998; Ong et al., 1996; Rabin et al., 1993). Whether the FRS2α-mediated signals are important for FGFR2 in control of prostate development and adult tissue homeostasis remains to be determined.

FRS2α is generally expressed in fetal and adult tissues (McDougall et al., 2001). Disruption of *Frs2α* alleles in early embryogenesis is lethal (Hadari et al., 2001). To circumvent this limitation and enable studies on later stages of development, we employed the loxP-Cre recombination system to inactivate *Frs2α* alleles in the prostate epithelium by crossing mice carrying loxP-flanked *Frs2α* (*Frs2α*^{flox}) (Lin et al., 2007b) and *Nkx3.1*^{Cre} knock-in alleles (Lin et al., 2007a). Similar to *Fgfr2* ablation, disruption of *Frs2α* in the prostate epithelium reduced epithelial cell proliferation, impaired branching morphogenesis during prostate development, and impaired post-puberty androgen-dependent prostate regeneration. Unlike *Fgfr2*^{cn} prostates, *Frs2α*^{cn} prostates remained strictly dependent on androgen with respect to tissue homeostasis. Ablation of *Frs2α* significantly inhibited the initiation and progression of autochthonous mouse prostate tumors. This indicated that FRS2α-mediated mitogenic signals are important for prostatic development and regeneration, and suggest a role of aberrant FRS2α-mediated signaling in prostate tumorigenesis.

MATERIALS AND METHODS

Animals

Mice carrying loxP-flanked *Frs2α* alleles, the *R26R-lacZ* reporter, and the *Nkx3.1*^{Cre} knock-in alleles were bred and genotyped as described (Jin et al., 2003b; Lin et al., 2007b; Soriano, 1999). Orchiectomy and androgen therapy were carried out as described previously (Lin et al., 2007a). All animals were housed in the Program for Animal Resources of the Institute of Biosciences and Technology, and were handled in accordance with the principles and procedures of the Guide for the Care and Use of Laboratory Animals. All experimental procedures were approved by the Institutional Animal Care and Use Committee.

Prostate cell and organ cultures

TRAMP-C2 cells were maintained in RD (50% RPMI, 50% DMEM) medium with 5% FBS as described (Foster et al., 1997). For protein stability analyses, the cells (1×10^6 cells in 10-cm dishes) were treated with 10 μg/ml cycloheximide for the indicated times. For FGF2 response analyses, the cells (1×10^5 in 6-well plates) were serum starved for 24 hours prior to being treated with 10 ng/ml FGF2 for 10 minutes.

Prostate tissues were dissected at postnatal day 0.5 as described (Lamm et al., 2001) and transferred to 0.4 μm Millicell-CM filters (Becton Dickinson Labware Europe, Meylan, France) inside 24-well tissue culture plates. Each well contained 0.5 ml of serum-free DMEM:Ham's F-12 (1:1) supplemented with 2% ITS (12.5 μg/ml insulin, 12.5 μg/ml transferrin, 12.5 ng/ml selenious acid), 2.5 μg/ml linoleic acid-albumin (Sigma, St Louis, MO), 25 μg/ml gentamycin, 0.25 μg/ml amphotericin B and 10 nM testosterone. PI3 kinase inhibitor (LY294002) and ERK1/2 inhibitor (Calbiochem, Darmstadt, Germany) were added to the medium at a final concentration of 10 μM where indicated. Cultures were maintained for 3 days at 37°C prior to harvest for analysis.

Histology

Prostates and prostate ducts were dissected and sectioned for histological analyses as previously described (Lin et al., 2007a). Main ducts and distal ductal tips were quantified from at least three animals. Data are presented as mean±s.d.

Hematoxylin and Eosin staining was performed on 5-μm sections; immunohistochemical analyses and in situ hybridization were performed on 7-μm sections mounted on Superfrost/Plus slides (Fisher Scientific, Pittsburgh, PA). The antigens were retrieved by autoclaving samples in 10 mM Tris-HCl buffer (pH 10.0) for 5-10 minutes or as suggested by manufacturers of the antibodies. The source and dilutions of primary antibodies are: mouse anti-cytokeratin 8 (1:15; Fitzgerald, Concord, MA); mouse anti-smooth muscle α-actin (1:1) and mouse anti-PCNA (1:1000) from Sigma (St Louis, MO); mouse anti-P63 (1:150), rabbit anti-FRS2α (1/500) and rabbit anti-androgen receptor (1:150) from Santa Cruz (Santa Cruz, CA); mouse anti-T antigens (1:500) from BD Pharmingen (Frankin Lakes, NJ); rabbit anti-phosphoAKT (1:500) and anti-phosphoERK1/2 (1:500) from Cell Signaling Technology (Danvers, MA); rabbit anti-probasin (1:3000) from the Greenberg laboratory (Fred Hutchinson Cancer Research Center, Seattle, WA); and rabbit anti-PSP94 (1:2000) from the Xuan laboratory (University of Western Ontario, London, Canada). The TSA Plus Fluorescein System from PerkinElmer (Shelton, CT) was used to visualize anti-FRS2α, anti-phosphoAKT and anti-phosphoERK1/2 antibodies and the ExtraAvidin Peroxidase System from Sigma to visualize all other antibodies. For whole-mount *lacZ* staining, the prostate tissues were lightly fixed with 0.2% glutaraldehyde for 30 minutes. *lacZ* staining was carried out by rocking in 1 mg/ml X-Gal at room temperature overnight as described (Liu et al., 2005).

For proliferation analyses in 1- and 2-week-old prostates, the percentage of PCNA-positive cells in the growing duct tips was determined, as most proliferating cells were located at the most-distal part of ducts at this stage. For 4-week-old and post-pubertal regenerating prostates, the percentage of PCNA-positive cells in the whole gland was determined, as the proliferating cells were randomly distributed in the whole gland. The data were collected from at least five slides per prostate, and three prostates per genotype, and are presented as mean±s.d.

Immunoblotting and analyses of secretory proteins

Dissected prostate tissues or TRAMP-C2 cells were homogenized in RIPA buffer (50 mM Tris-HCl buffer pH 7.4, 1% NP40, 150 mM NaCl, 0.25% Na-deoxycholate, 1 mM EGTA, 1 mM PMSF), and extracted soluble proteins were harvested by centrifugation. Samples containing 50 μg protein were separated by SDS-PAGE and electroblotted onto nylon membranes for western analyses with the indicated antibodies. The dilutions of the antibodies are: anti-phosphoFRS2α, 1:1000; anti-phosphoERK1/2, 1:1000; anti-phosphoAKT, 1:1000; anti-AKT, 1:1000; anti-FRS2α, 1:1000; anti-ERK1/2, 1:3000; and anti-FGFR2, 1:1000. For immunoprecipitation, soluble tissue lysates containing 500 μg protein were incubated with 2 μg of the indicated antibodies overnight, and then the immunocomplexes associated with 10 μl protein A-Sepharose beads were collected by centrifugation and extracted with SDS sample buffer for western analyses. The specific bands were visualized using the ECL-Plus chemoluminescent reagents. The films were scanned with a densitometer and the bands quantified using Image J software (NIH).

Secretory proteins were extracted as described (Lin et al., 2007a). The protein concentrations were determined and adjusted to a final concentration of 1 mg/ml with PBS. Samples containing 25 μg protein were separated by 5-20% gradient SDS-PAGE and visualized by Coomassie Blue staining. Samples of 50 μg protein were used for western blotting analyses with anti-probasin or anti-PSP94 as indicated.

Gene expression

For in situ hybridizations, paraffin-embedded tissue sections were rehydrated, followed by 20 μg/ml protease K digestion for 7 minutes at room temperature. After prehybridization at 65°C for 2 hours, the hybridization was carried out by overnight incubation at 65°C with 0.5 μg/ml digoxigenin-labeled RNA probes for the indicated genes. Non-specifically bound probes were removed by washing four times with 0.1×DIG washing buffer at 60°C for 30 minutes. Specifically bound probes were detected using alkaline phosphatase-conjugated anti-digoxigenin antibody (Roche, Indianapolis, IN).

For real-time RT-PCR analyses, total RNA was extracted from prostates using the RiboPure Kit (Ambion, Austin, TX). The first-strand cDNAs were reverse transcribed from the RNA template using SuperScript II reverse transcriptase (Invitrogen, Carlsbad, CA) and random primers according to manufacturer's protocols. Real-time PCR analyses were carried out using the SYBR Green JumpStart Taq Ready Mix (Sigma) as instructed by the manufacturer. Relative abundances of mRNA were calculated using the comparative threshold (CT) cycle method and were normalized to β-actin or 18S rRNA as an internal control. The mean and s.d. among at least three individual experiments are shown. RT-PCR products were analyzed on 2% agarose gels for validation of products by size.

RESULTS

Disruption of *Frs2α* alleles specifically in the prostate epithelium

Previously, we reported that FGFR2 signaling is important for prostate development and acquisition of androgen responsiveness. To determine whether *Frs2α*, a receptor-proximal adaptor in FGF signaling, was essential for prostatic development, the loxP-Cre recombination system was used to conditionally inactivate *Frs2α* alleles in prostatic epithelial cell precursors (Fig. 1A). Mice carrying homozygous $Frs2\alpha^{cn}$ alleles were viable and fertile. Disruption of the *Frs2α* in prostates was confirmed by PCR (Fig. 1B). Real-time RT-PCR analyses revealed that expression of *Frs2α* in 1-week-old $Frs2\alpha^{cn}$ prostates was significantly reduced compared with the control prostates (Fig. 1C).

Frs2α expression was further characterized by in situ hybridization with *Frs2α*-specific probes. The results showed that although *Frs2α* expression was constant in the stromal compartment, it exhibited a spatial and temporal expression pattern in the epithelium (Fig. 1D). In 1-week-old prostates, *Frs2α* was expressed relatively uniformly at high levels in the epithelium. In 2-week-old prostates, the expression became restricted to cells located at distal tips of the ductal network, where the cells were actively engaged in proliferation. In the prostates of mice at 4 weeks or older, expression of *Frs2α* was limited to basal epithelial and stromal cells. No *Frs2α* expression was detected in luminal epithelial cells. Ablation of *Frs2α* with $Nkx3.1^{Cre}$ diminished *Frs2α* expression in the epithelial compartment of prostates, including basal and luminal epithelial cells (Fig. 1D), whereas *Frs2α* expression in the stromal cells remained intact. Thus, the basal level of *Frs2α* expression indicated by RT-PCR in prostates of $Frs2\alpha^{cn}$ and 4-week-old control mice was a constitutive property of stromal and basal cells.

Unlike $Fgfr2^{cn}$ prostates that only have dorsal and lateral lobes, $Frs2\alpha^{cn}$ prostates were relatively normal and consisted of anterior, dorsal, lateral and ventral prostate (AP, DP, LP and VP, respectively) lobes, although these were smaller and more transparent than wild-type prostates (see Fig. S1A in the supplementary material). The prostates of genotype $Frs2\alpha^{flox/flox}$, $Frs2\alpha^{flox/WT}$, $Frs2\alpha^{flox/cn}$, $Frs2\alpha^{WT/WT}$ or $Nkx3.1^{Cre}$, had no noticeable differences in organ morphology and histological structures, and were all considered as control prostates.

Ablation of *Frs2α* alleles in the prostate epithelium inhibits prostatic branching morphogenesis and growth

To improve direct visualization of branching morphogenesis, the *R26R-lacZ* reporter allele was introduced into the $Frs2\alpha^{cn}$ mice by crossing with mice bearing a *lacZ* reporter silenced by a loxP-flanked sequence (Soriano, 1999). Activation of the *R26R-lacZ* reporter by the Cre recombinase occurred concurrently with disruption of the $Frs2\alpha^{flox}$ alleles in the same cells. Whole-mount staining with X-Gal showed that similar to $Fgfr2^{cn}$ embryos, prostatic buds formed at E17.5 in $Frs2\alpha^{cn}$ embryos with no apparent difference to controls. Although all mutant buds formed AP, DP, LP and VP lobes, fewer ductal branches were observed in the $Frs2\alpha^{cn}$

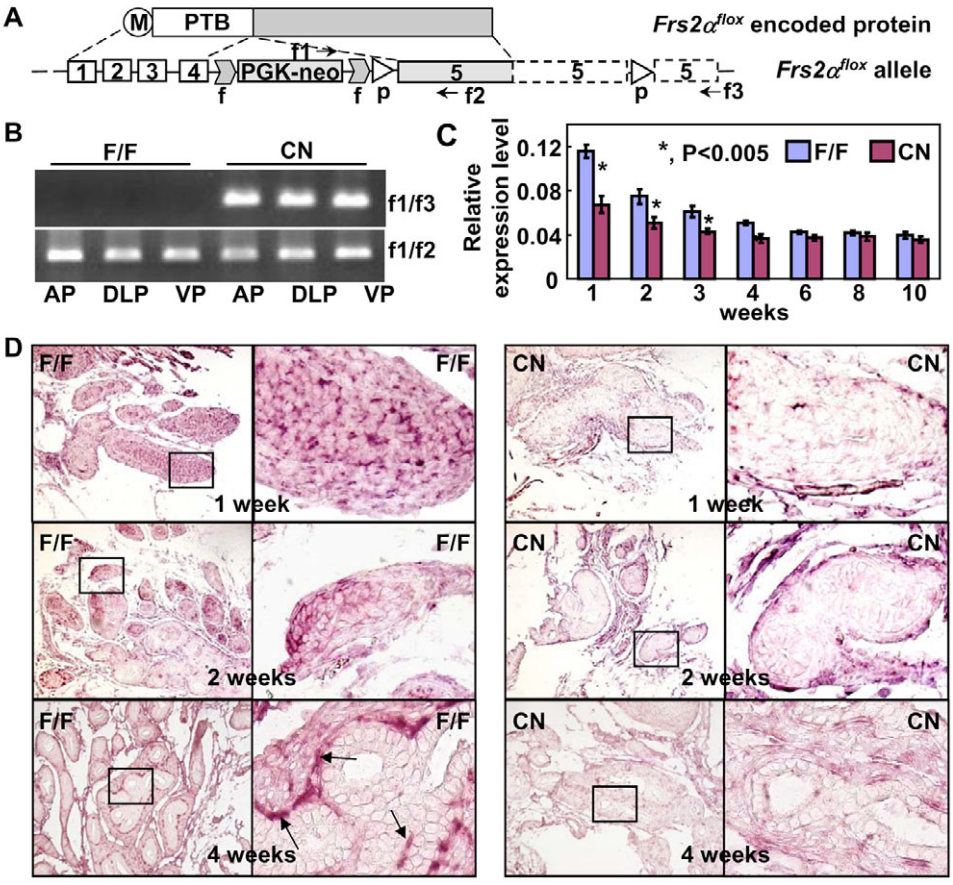

Fig. 1. Disruption of *Frs2α* alleles in prostate epithelium. (**A**) Schematic of the floxed *Frs2α* alleles for conditional disruption. The genomic DNA containing coding exons 1-5 and adjacent introns is shown. Dashed boxes indicate non-coding exon sequence. The primers for PCR genotyping are indicated by arrows. Primers f1 and f2 amplify a 319 bp fragment from the floxed *Frs2α* allele. Primers f1 and f3 amplify a 261 bp fragment from the *Frs2α*-null allele; no amplification from wild-type alleles. (**B**) PCR genotyping for the *Frs2α* conditional-null alleles. Genomic DNAs extracted from each prostatic lobe of 4-week-old mice were analyzed by PCR using the primers illustrated in A. (**C**) Total RNAs were extracted from prostates of different ages, and *Frs2α* expression was assessed by real-time RT-PCR. The data were normalized to β-actin loading controls and are expressed as mean±s.d. of at least three independent experiments. Note that *Frs2α* alleles were intact in the stromal compartment, which is likely to account for the basal level of *Frs2α* expression in $Frs2\alpha^{cn}$ prostates. Representative data from dorsolateral prostate are shown. (**D**) In situ hybridization of *Frs2α* expression in prostates. Enlarged image of boxed area shown on the right. Note that the expression was diminished in the epithelium of $Frs2\alpha^{cn}$ prostates and mature control prostates. Arrows indicate basal cells. AP, anterior prostate; DLP, dorsolateral prostate; VP, ventral prostate; M, myristylation site; PTB, phosphotyrosine-binding site; f, Frt element; p, loxP element; F/F, homozygous $Frs2\alpha^{flox}$ mice; CN, $Frs2\alpha^{cn}$ mice.

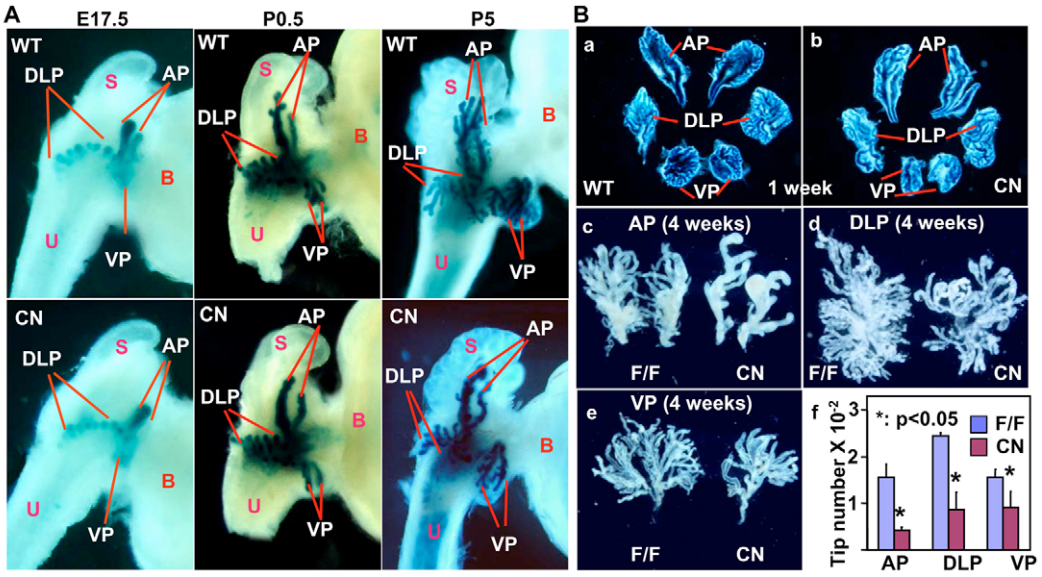

Fig. 2. Disruption of *Frs2α* alleles inhibits ductal branching morphogenesis in prostates. (**A**) The urogenital tract was dissected at the indicated times, lightly fixed and then stained with X-Gal. Stained tissues representing each prostatic lobe are shown. Note the lack of significant differences between *Frs2α*^{cn} (below) and control (above) prostate rudiments at E17.5 or later. (**B**) Prostatic lobes were dissected from mice at the indicated ages. The tissues were lightly fixed and stained with X-Gal (**a**,**b**). Note that only epithelial cells in the prostate were stained. The ductal network in each prostatic lobe from 4-week-old mice was microdissected (**c-e**) and the average number of tips was quantified from three prostates and is shown as mean±s.d. (**f**). AP, anterior prostate; DLP, dorsolateral prostate; VP, ventral prostate; B, bladder; S, seminal vesicles; U, urethra; F/F, homozygous *Frs2α*^{flox} mice; CN, *Frs2α*^{cn} mice; WT, wild-type *Frs2α*.

prostates than in controls (Fig. 2A). We then dissected each prostatic lobe from 1-week-old mice to examine the *Frs2α*^{cn} prostates in more detail. The X-Gal stain confirmed that that the complexity of the ductal network in the *Frs2α*^{cn} prostates was reduced. Quantitative analyses of ducts microdissected out of 4-week-old prostates revealed a reduction in the number of ductal tips in every lobe of the *Frs2α*^{cn} prostates (Fig. 2B). This indicated that the extent of branching morphogenesis, but not budding, was compromised in *Frs2α*^{cn} prostates.

To determine whether FRS2α protein was carried over into mutant prostatic buds after ablation of expression by the *Nkx3.1*^{Cre}-mediated recombination, the prostate rudiments at different stages were assessed with an anti-FRS2α antibody. FRS2α was strongly expressed in epithelial cells of control prostate rudiments and the expression gradually declined with development of the prostate. Although *Nkx3.1*^{Cre} is expressed prior to E17.5, FRS2α protein remained evident in mutant epithelial cells at E18.5 and then diminished at the neonatal stage (Fig. 3A). The number of cells positive for P63 (also known as Trp63 – Mouse Genome Informatics) remained relatively constant over the same period with a slight decrease in *Frs2α*^{cn} prostates at later stages (Fig. 3B). Most epithelial cells in normal prostate rudiments expressed P63 (Pu et al., 2007). This indicated a persistence of FRS2α protein beyond ablation of expression. Separate experiments in vitro indicated that the half-life of FRS2α was longer than that of FGFR2 in prostate epithelial tumor cells (Fig. 3C,D). These results indicated that the carryover of FRS2α after ablation by recombination might be sufficient to participate in signals that support prostatic bud formation in early prostate morphogenesis.

Presence of the proliferating cell nuclear antigen (PCNA) showed that the number of proliferating cells in *Frs2α*^{cn} distal tips was reduced compared with controls at 1-2 weeks of age (Fig. 4A,B). At 3-4 weeks, the prostates were undergoing rapid growth associated with puberty. The proliferating cells were widely distributed across the prostates. Proliferation in whole dorsolateral prostate (DLP) and AP lobes in *Frs2α*^{cn} prostates was also lower than in the controls (Fig. 4A,B). Post-puberty cell proliferation at 6 weeks in both *Frs2α*^{cn} and control prostates was dramatically reduced. No difference was observed between *Frs2α*^{cn} and control prostates at this stage (data not shown). Together, the results demonstrate that FRS2α-mediated signals are important for prostate cell proliferation during development. Since these results mirror the *Fgfr2* ablation, they suggest a role of FRS2α in mediating FGFR2 mitogenic signals in the epithelial cells during prostate development.

The expression of 22 key regulatory genes was compared between control and *Frs2α*^{cn} 1-week-old prostates by real-time RT-PCR. The *Frs2α*^{cn} prostates exhibited reduced expression of BMP7, HOXb13, HOXd13 and NKX3.1 and increased expression of FGFR4. No significant difference was observed between *Frs2α*^{cn} and control prostates in the expression of the other genes tested (Fig. 4C). HOXb13, HOXd13 and NKX3.1 are highly expressed in luminal epithelial cells and play a role in differentiation of luminal epithelial cells (Economides and Capecchi, 2003). The results suggest that in addition to its effects on proliferation and branching morphogenesis, ablation of FRS2α might also compromise luminal epithelial cell differentiation.

Ablation of *Frs2α* reduces activation of MAP kinase in prostatic epithelial cells

As an adaptor, FRS2α has multiple binding sites for downstream substrate that are required for FGFR to activate the MAP kinase and AKT pathways (Gotoh et al., 2004; Ong et al., 2000; Xu and Goldfarb, 2001). To determine whether FRS2α-mediated signals activate the MAP kinase and AKT pathways, prostates were harvested from mice at 1, 2 and 4 weeks of age and subjected to immunoblot analysis of activated FRS2α, ERK1/2 (also known as

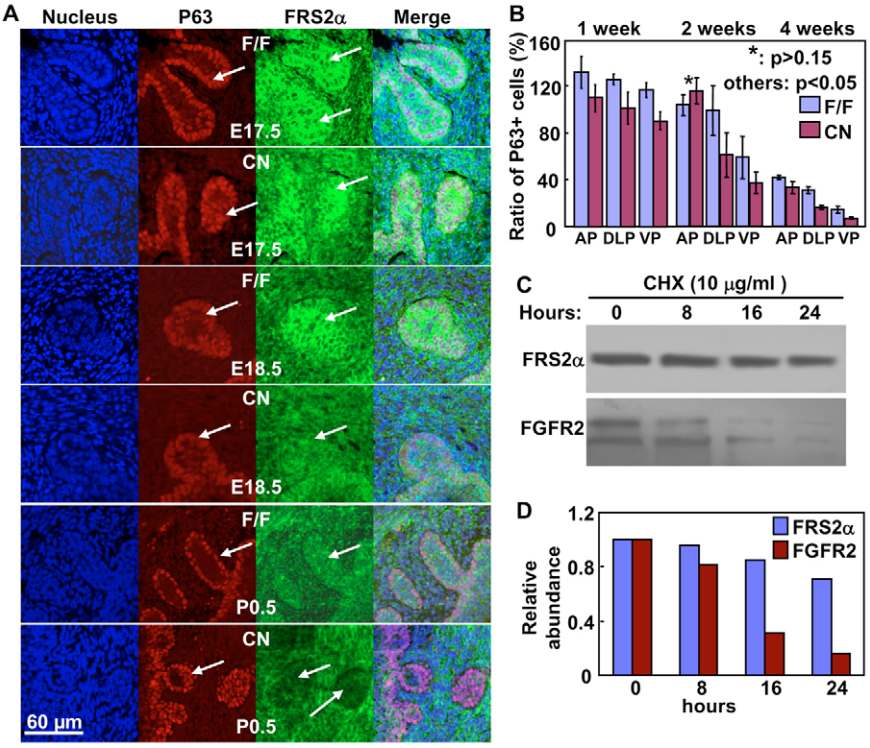

Fig. 3. Depletion of FRS2α proteins in *Frs2α*^{cn} prostatic rudiments. (**A**) Prostates were collected at the indicated times, immunostained with the indicated antibodies, and visualized by confocal microscopy. The prostate epithelial cells were identified with anti-P63 antibody. Expression of FRS2α was assessed with anti-FRS2α antibody. Arrows indicate prostate epithelial cells. Note that FRS2α staining was diminished in *Frs2α*^{cn} prostates at postnatal day 0.5 (P0.5). (**B**) The ratio of p63-positive cells in the epithelial compartment at different ages was calculated from three samples. Representative mean±s.d. values of data from triplicate samples are shown. (**C**,**D**) Stability of FRS2α proteins as compared with FGFR2 in prostate epithelial cells. TRAMP-C2 cells (1×10^6) treated with cycloheximide were lysed at the indicated times. The abundance of FRS2α was analyzed by western blot directly from the cell lysates (containing 50 μg protein). FGFR2 in cell lysates (containing 500 μg protein) was pulled down with anti-FGFR2 antibody. The specifically bound fractions were subjected to western analyses (C). The specific bands were quantitated with a densitometer and the data presented as ratios of treated to non-treated cells (D). CHX, cycloheximide; F/F, homozygous *Frs2α*^{flox} mice; CN, *Frs2α*^{cn} mice.

MAPK3/1 – Mouse Genome Informatics) and AKT (also known as AKT1 – Mouse Genome Informatics). FRS2α was strongly expressed and phosphorylated in 1-week-old normal prostates relative to diminished levels in 4-week-old prostates (Fig. 5A). Coincident with changes in FRS2α, phosphorylation of ERK1/2 in the control prostates was strong in early development and diminished at later stages. By contrast, phosphorylation of AKT was relatively constant. Ablation of *Frs2α* reduced the phosphorylation of ERK, but not AKT (Fig. 5A,B). Immunohistochemical analysis of tissues using anti-phosphorylated ERK1/2 (Fig. 5C) and anti-phosphorylated AKT antibodies (Fig. 5D) confirmed the immunoblot results. In contrast to *Frs2α* ablation, ablation of *Fgfr2* reduced both ERK1/2 and AKT phosphorylation in addition to the expected reduction in

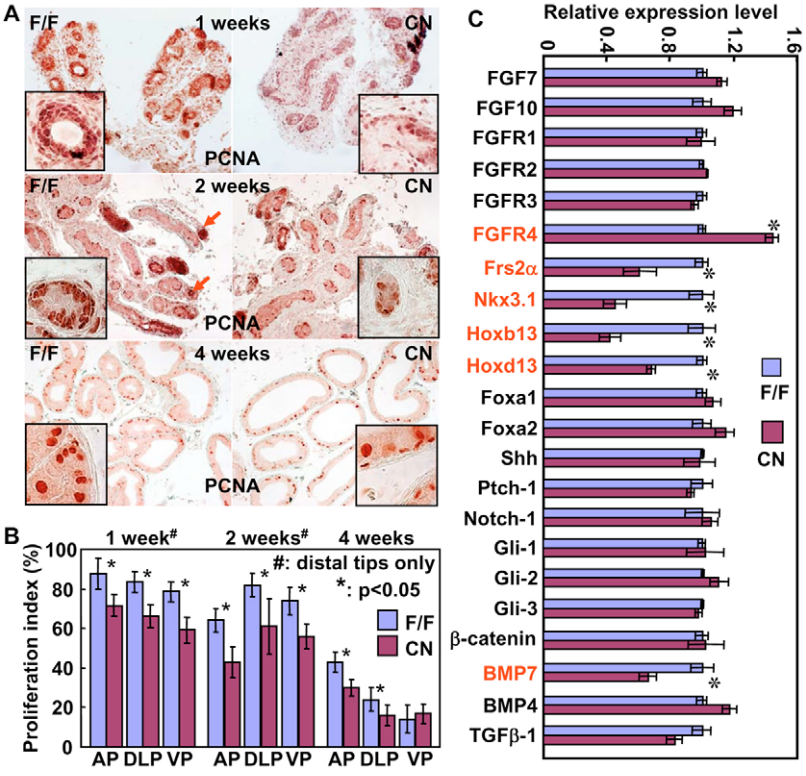

Fig. 4. Compromised proliferation in *Frs2α*^{cn} prostates during prepubertal and pubertal growth stages. (**A**) Prostate tissues were collected from control and mutant mice at the indicated ages and proliferating cells assessed by immunostaining for PCNA. Note that the proliferating cells mainly reside at the distal tips of the ductal network in 1- or 2-week-old prostates, but are randomly distributed in 4-week-old prostates of both control and mutant mice. Arrows indicate proliferating tips. Representative data from the dorsolateral prostate are shown. Insets are high-magnification views from the same sections. (**B**) PCNA-stained cells in distal tips of 1- or 2-week-old prostates, or whole prostate (4 weeks old), were scored. The ratio of PCNA-positive to total epithelial cells was calculated from five sections per prostate. Mean±s.d. values of data from three prostates are shown. (**C**) Real-time RT-PCR analyses of RNAs encoding the indicated genes from 1-week-old prostates. Data were normalized to β-actin loading controls and then presented as the relative difference to the control prostates. Mean±s.d. values of data from three prostates are shown. AP, anterior prostate; DLP, dorsolateral prostate; VP, ventral prostate; F/F, homozygous *Frs2α*^{flox} mice; CN, *Frs2α*^{cn} mice.

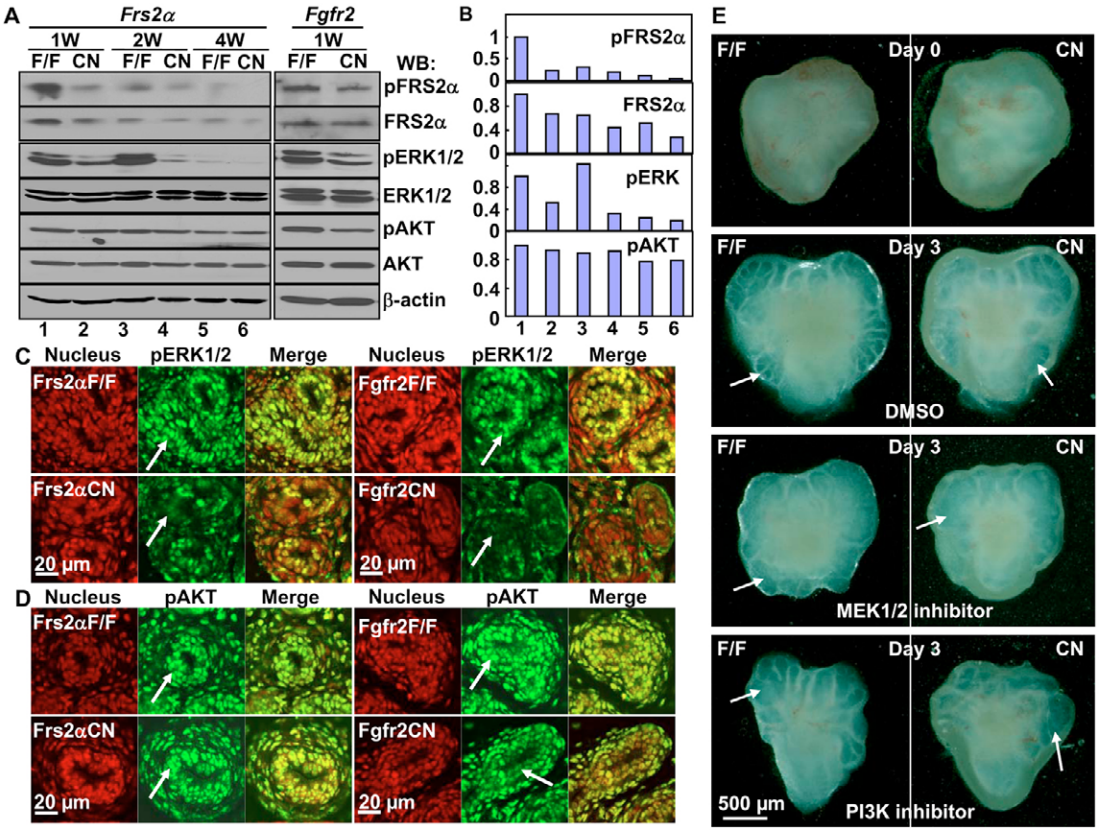

Fig. 5. Activation of the MAP kinase pathway is compromised in *Frs2α*^{cn} prostates during branching morphogenesis. (**A**,**B**) Western analyses (A) of the indicated proteins from Triton-extracts of mouse prostates at the indicated ages. β-actin was used as a loading control. Note that phosphorylated FRS2α and ERK1/2 were prominent in 1- and 2-week-old prostates and were diminished in 4-week-old prostates, whereas phosphorylated AKT remained constant in the prostates. The specific bands were quantitated (B) by densitometry. (**C**,**D**) Immunostaining of phosphorylated ERK1/2 (C) and phosphorylated AKT (D) in tissue sections of 1-week-old prostates. The specific staining was visualized with confocal microscopy. Note that phosphorylated ERK1/2 was reduced in the epithelial cells, but not in the stromal cells, of *Frs2α*^{cn} prostates, and that both phosphorylated ERK1/2 and phosphorylated AKT were reduced in epithelial cells of *Fgfr2*^{cn} prostates. Arrows indicate epithelial cells. (**E**) Newborn prostate rudiments cultured with 10 μM ERK1/2 (MEK1/2) or PI3 kinase inhibitor, as indicated, for 3 days. Arrows indicate lumens of the prostatic ductal structures. pERK1/2, phosphorylated ERK1/2; pAKT, phosphorylated AKT; F/F, homozygous *Frs2α*^{flox} mice; CN, *Frs2α*^{cn} mice.

phosphorylation of FRS2α (Fig. 5A,C,D). These results suggest that FGFR2 is a major source of FRS2α activation in prostate epithelial cells during development, and that activation of the MAP kinase pathway, but not the AKT pathway, by FGFR2 is likely to be mediated by FRS2α in prostates.

ERK1/2 inhibitors in organ culture of newborn prostates were employed to test whether inhibition of the MAP kinase pathway mimicked the FRS2α deficiency with respect to prostatic branching morphogenesis. Similar to tissue from *Frs2α*^{cn} prostates, normal prostate tissue treated with the inhibitors exhibited decreased ductal complexity indicative of compromised branching morphogenesis of prostatic buds (Fig. 5E). However, inhibition of ERK1/2 did not further decrease the ductal complexity of *Frs2α*^{cn} prostates, implying that the FRS2α-mediated pathway is the major activator of the MAP kinase pathway during prostate branching morphogenesis. PI3 kinase inhibitors also significantly reduced the extent of ductal differentiation, similar to the effect of MAP kinase inhibitors. This suggests that both MAP and PI3 kinase pathways are important for prostate branching morphogenesis, but that FRS2α is primarily an effector of FGFR2 kinases for activating the MAP kinase pathway without compromise of the PI3 kinase pathway in prostate epithelial cells.

Frs2α ablation compromises androgen-induced prostatic cell proliferation without effect on androgen-dependent secretory function

Although *Frs2α*^{cn} prostates were smaller overall, they exhibited a similar epithelial infolding to normal wild-type prostates (see Fig. S1 in the supplementary material). No significant difference was observed in the display of luminal cell cytokeratin 8 (also known as keratin 8 – Mouse Genome Informatics), or α-actin in stromal cells, or androgen receptor (AR) in both luminal epithelial and stromal cells, between *Frs2α*^{cn} and control prostates (see Fig. S2A in the supplementary material). *Frs2α*^{cn} prostates exhibited near-normal levels of secretory proteins, although some reduction in the production of probasin and PSP94 (also known as MSMB – Mouse Genome Informatics) was noted in the VP lobe (see Fig. S2B,C in the supplementary material).

Previously, we reported that ablation of the *Fgfr2* alleles interfered with the strict androgen-dependent properties of prostate with respect to tissue homeostasis. To test whether ablation of *Frs2α* exhibited a similar effect, 8-week-old mice were deprived androgens by orchiectomy. Similar to the effect on control prostates, the androgen deprivation induced apoptosis in *Frs2α*^{cn} prostates within 2 days (data not shown) and the tissues atrophied in 2 weeks (see

Fig. S3 in the supplementary material). This is in marked contrast to *Fgfr2*^{cn} prostates, which remained largely unresponsive to the same androgen deprivation after 2 weeks (Lin et al., 2007a). This suggested that resident epithelial cell FGFR2 instructed the prostate to acquire strict dependence on androgen via pathways other than those mediated by FRS2α.

During regeneration induced by restoration of androgen, expression of FRS2α was apparent in the restored prostate luminal epithelial cells (Fig. 6A). Real-time RT-PCR analyses confirmed that *Frs2α* expression was significantly increased in regenerating prostates as compared with the castrated remnants (Fig. 6B). This suggested that FRS2α plays a role in prostate regeneration. To test this, the rate of epithelial cell proliferation was compared among normal, FRS2α and FGFR2-deficient regenerating prostates induced by androgen. PCNA immunostaining of proliferating cells revealed that, similar to the effect of *Fgfr2* ablation, disruption of *Frs2α* significantly reduced proliferation activity in the prostate epithelium (Fig. 6). Taken together, the results indicate that FRS2α potentially mediates mitogenic signals of FGFR2 during androgen-induced proliferation, but FGFR2 support of androgen-dependent gene expression in the prostate is mediated by FRS2α-independent pathways.

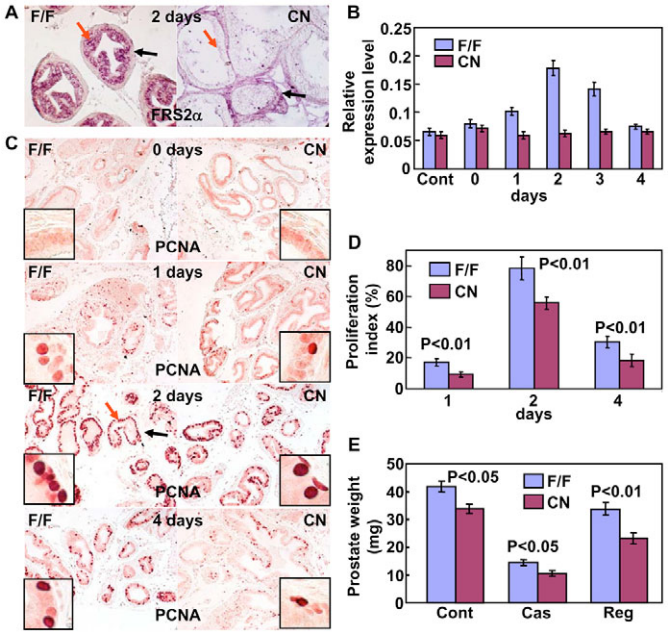

Fig. 6. Compromised proliferation activities in regenerating *Frs2α*^{cn} prostates induced by androgens. (**A**,**B**) Expression of *Frs2α* in the epithelium of regenerating prostates. Expression of *Frs2α* was assessed by in situ hybridization (A) or real-time RT-PCR (B). Data were normalized to the abundance of 18S rRNA and are expressed as mean±s.d. of at least three prostates. The background of *Frs2α* expression in the conditional mutants is from the stroma. Red arrows, epithelial cells; black arrows, stromal cells. (**C**,**D**) Reduced androgen-induced proliferation in *Frs2α*^{cn} prostates. Androgen was restored to mice 14 days after orchiectomy to induce prostate regeneration. Tissues were harvested at the indicated days after administration of androgen. Proliferating cells were revealed by immunostaining with anti-PCNA antibody (C). Red arrows, epithelial cells; black arrows, stromal cells. (D) Representative data from the dorsolateral prostate are shown. PCNA-positive cells were scored and reported as ratios of proliferating cells to total cell numbers. Mean±s.d. values of data from at least three prostates are shown. (**E**) The average wet tissue weights of normal prostates before castration (Cont), 2 weeks after the operation (Cas), and 14 days after administration of androgen (Reg). Mean±s.d. values of data from three samples are shown. F/F, homozygous *Frs2α*^{flox} mice; CN, *Frs2α*^{cn} mice.

Ablation of *Frs2α* in the prostatic epithelium inhibits prostatic tumorigenesis

Although FRS2α was not expressed in luminal epithelial cells of mature normal prostates, it appeared prominently in luminal epithelial cells in prostate tumors in the TRAMP mouse (Fig. 7A,B), the tumors of which were induced by oncogenic T antigens targeted to prostate epithelial cells (Kaplan-Lefko et al., 2003). This was coincident with the ectopic appearance of FGFR1 in foci of high-grade PIN and overt tumor cells in the TRAMP prostates (Fig. 7A). These results are consistent with the previous finding that the ectopic appearance of normally stromal resident FGFR1 is often associated with prostate tumor progression (Jin et al., 2003a; Kwabi-Addo et al., 2001). The significantly increased phosphorylation of FRS2α, ERK1/2 and AKT in TRAMP-C2 epithelial cell lines derived from the TRAMP tumors induced by FGF2, indicated the presence of active ectopic FGFR1 signaling in the tumor cells (Fig. 7C). TRAMP-C2 cells are characterized by expression of ectopic FGFR1 (Foster et al., 1999). FGF2 is specifically recognized by ectopic FGFR1, but not by resident FGFR2IIIb, in prostate epithelial cells (McKeehan et al., 1998). Thus, it is likely that FRS2α plays a role in mediation of ectopic FGFR1 in prostate tumors.

To determine whether FRS2α had any impact on tumorigenesis in the TRAMP mice, the *Frs2α*^{cn} and TRAMP mice were crossed. Histological analysis showed that by 10 weeks, the majority of TRAMP mice carrying the floxed *Frs2α* alleles developed the expected low-to-high-grade PIN lesions. PIN foci were apparent across the whole prostate with an estimated 80% of the prostate exhibiting various degrees and grades of PIN lesions (Fig. 7D,E). Although the TRAMP transgenic T antigens were highly expressed in the *Frs2α*^{cn} prostates, PIN lesions across the *Frs2α*^{cn} prostates were fewer in number and the majority of the lesions were lower grade than in control TRAMP mice (Fig. 7D,E). By 24 weeks, most control TRAMP mice developed advanced, poorly differentiated tumors, whereas tumors in the *Frs2α*^{cn}/TRAMP hybrids were well-differentiated (Fig. 7D). Application of a Kaplan-Meier survival analysis showed that ablation of *Frs2α* alleles significantly increased the life span of TRAMP mice (Fig. 7F). These results strongly suggest that ablation of FRS2α-mediated signaling pathways in prostate epithelial cells inhibits prostate tumor initiation and progression in the TRAMP mice. and this mostly likely occurs through the adaptor function of FRS2α with ectopic FGFR1.

DISCUSSION

Disruption of *Frs2α* in prostate epithelium impairs prostatic morphogenesis

Members of the FGF family play cell-specific roles in prostatic development, function, compartmental homeostasis and tumorigenesis (Lin et al., 2007a; McKeehan et al., 1998). Here we report that the expression of FRS2α, a major adaptor protein in the FGF signaling cascade, is spatiotemporally expressed and is closely associated with prostatic cell proliferation. Although diminished in the adult prostatic epithelium, expression of FRS2α was activated in epithelial cells of regenerating and tumor prostates. Tissue-specific ablation of *Frs2α* in prostatic epithelial precursor cells compromised prostatic branching morphogenesis and growth. Furthermore, ablation of *Frs2α* alleles retarded prostatic tumor formation and progression in the autochthonous TRAMP mouse

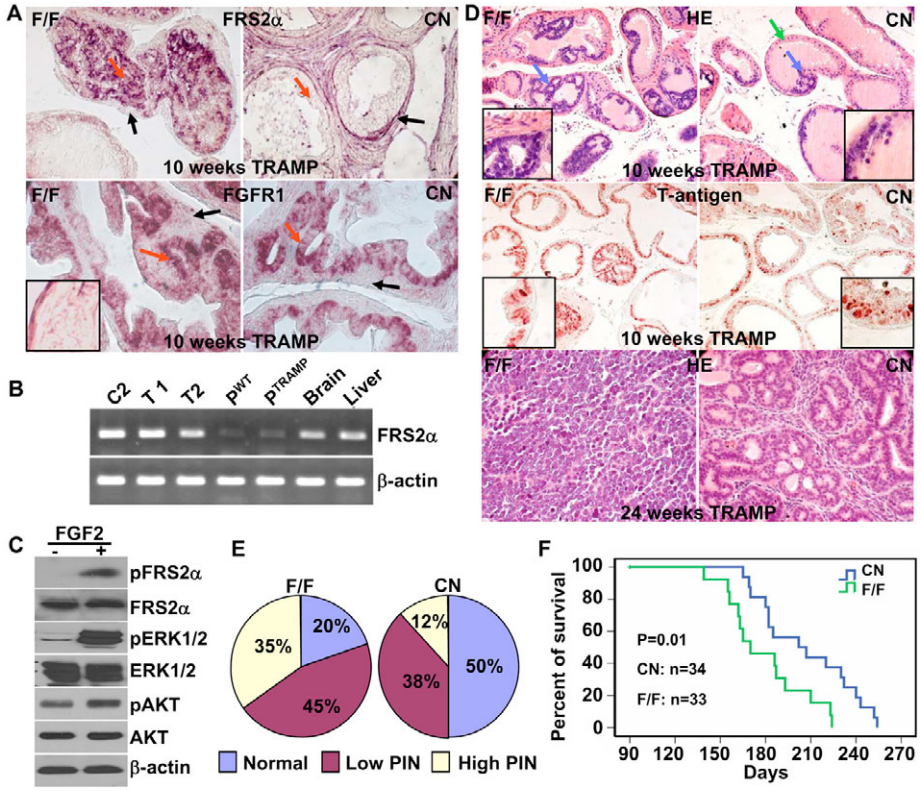

Fig. 7. Ablation of FRS2α in the prostatic epithelium inhibits tumorigenesis in the TRAMP prostatic tumor model. (**A**,**B**) Expression of *Frs2α* and *Fgfr1* at the mRNA level was assessed in TRAMP prostates by in situ hybridization (A) and RT-PCR (B). Red arrows, epithelial cells; black arrows, stromal cells. Inset, wild-type control showing no expression of *Fgfr1* in the epithelial compartment. T1 and T2, different, individual TRAMP tumors; C2, the C2 cell line derived from TRAMP tumors; P^{WT}, prostates of 6-month-old wild-type mice; P^{TRAMP}, prostates of 3-week-old TRAMP mice in which PIN lesions are minimal. Brain and liver were used as positive controls; β-actin as a loading control. (**C**) Treatment of TRAMP-C2 cells with FGF2 (10 ng/ml) for 10 minutes after serum starvation for 24 hours. Cells were lysed and the lysates analyzed by western blot with the indicated antibodies. (**D**) Prostate tissue sections were prepared from TRAMP mice with homozygous *Frs2α*-null or *Frs2α* floxed alleles at the indicated ages and stained with Hematoxylin and Eosin (HE) or analyzed by immunohistotaining with anti-T-antigen antibody. Blue arrows, focal lesions; green arrows, normal epithelial cells. (**E**) PIN foci in prostates of 10-week-old TRAMP mice were identified as defined (Park et al., 2002), and the percentage area occupied by lesions quantitated. Mean±s.d. values of data from five prostates are shown. (**F**) Mortality of TRAMP mice with the indicated *Frs2α* alleles was determined from daily observation over 250 days. The percentage of mice that survived to the indicated ages is shown. pFRS2α, phosphorylated FRS2α; pERK1/2, phosphorylated ERK1/2; pAKT, phosphorylated AKT; F/F, homozygous TRAMP-$Frs2\alpha^{flox}$ mice; CN, TRAMP-$Frs2\alpha^{cn}$ mice.

model of prostate cancer. The data demonstrate that FRS2α is important for prostatic development and growth, and imply that aberrant activation of FRS2α-mediated signaling might contribute to prostatic tumorigenesis.

FRS2α in mediation of the FGF10/FGFR2 signals for prostate development and growth

During prostatic organogenesis, FGF7 and FGF10 are expressed in the mesenchyme, and FGFR2IIIb, the cognate receptor for FGF7/10, is expressed in the epithelium of the distal parts of elongating and branching ducts in prostatic rudiments (Huang et al., 2005; Thomson and Cunha, 1999). Ablation of FGFR2 in prostate epithelial cell precursors inhibits cell proliferation and cellularity throughout prostatic development (Lin et al., 2007a). Because of its role as a general adaptor bridging activated FGFR kinases and the MAP kinase, ablation of *Frs2α* potentially compromises activity of the FGF7/10-FGFR2IIIB axis. Together with the data showing that ablation of *Fgfr2* concurrently reduced activation of FRS2α and the MAP kinase pathway, the results suggest that FGFR2 signals for activating the MAP kinase pathway and regulating cell proliferation in prostate epithelial cells were mediated by FRS2α. By contrast, phosphorylated AKT was reduced in $Fgfr2^{cn}$, but not in $Frs2\alpha^{cn}$, prostates (Fig. 5). This indicates that FGFR2 activates the AKT pathway via an FRS2α-independent mechanism. Unlike *Fgfr2* ablation, which abrogates anterior and ventral prostatic bud formation, ablation of FRS2α did not disrupt development of prostatic buds. It is not uncommon that the prostate has a lobe-specific response to morphoregulatory genes (Economides and Capecchi, 2003; Podlasek et al., 1997; Pu et al., 2007). Because the apparent half-life of FRS2α is longer than that of FGFR2, our results could not resolve whether FGFR2 signals in prostatic bud formation were mediated by FRS2α-independent pathways or by the carryover of FRS2α. Further experiments are needed to clarify this issue.

Several signaling pathways, including those of SHH, Notch, BMP and FGF, have been implicated in prostate development. Ablation of *Frs2α* or *Fgfr2* alleles reduced expression of HOXd13. In addition, ablation of *Frs2α* reduced expression of BMP7 and HOXb13 and increased expression of FGFR4, FGF7, FGF10 and BMP4. Of this set of regulators, ablation of *Fgfr2* reduces expression of BMP4 (Lin et al., 2007a). This difference suggested that FGFR2 signaling in prostate epithelial cells is at least in part mediated by FRS2α, but that FGFR2 is not the only upstream activator of FRS2α in the prostate. Notably, HOXb13 is only expressed in ventral prostates. Concurrent inactivation mutations of both *Hoxb13* and *Hoxd13* cause severe hypoplasia in ventral prostate morphogenesis (Economides and Capecchi, 2003). Our results suggest that both *Hoxb13* and *Hoxd13* might be downstream targets of FRS2-mediated signaling cascades in the prostate, and that FRS2α-mediated signals are crucial for ventral epithelial cell differentiation. The expression of PSP94 and probasin, which are secretory proteins characteristic of mature luminal epithelial cells, was consistently and significantly reduced in $Frs2\alpha^{cn}$ ventral prostate (see Fig. S2B in the supplementary material). These results suggest that ablation of *Frs2α* compromises luminal epithelial cell differentiation in ventral prostate. Further experiments will be carried out to test this possibility.

Knock-in of the Cre cDNA to the *Nkx3.1* locus disrupts one *Nkx3.1* allele. Consistent with an earlier report that verified reduced expression of *Nkx3.1* in heterozygous *Nkx3.1*-null prostates (Bhatia-Gaur et al., 1999), our results showed a reduction in expression of *Nkx3.1* in $Frs2\alpha^{cn}$ prostates. By contrast, expression of *Nkx3.1* in $Fgfr2^{cn}$ prostates that also carry only one *Nkx3.1* allele remained similar to that in controls (Lin et al., 2007a). Others reported that *Nkx3.1* expression in prostate is regulated both by androgen and FGF signaling pathways (Pu et al., 2007). Thus, it is possible that expression of *Nkx3.1* is repressed by FGFR2 via FRS2α-independent pathways and that the repression is alleviated upon ablation of FGFR2 and to a degree sufficient to result in a net expression of *Nkx3.1* equal to that of wild-type prostates. It is also possible that loss of FGFR2 activates the non-canonical expression of *Nkx3.1*.

Ablation of *Frs2α* alleles attenuates androgen-induced prostatic regeneration

Ablation of *Fgfr2* alleles compromises the acquisition of dependence of the prostate on androgen with respect to tissue homeostasis. By contrast, FRS2α-deficient prostates remained strictly androgen-dependent. Similar to controls, $Frs2\alpha^{cn}$ prostates responded to androgen deprivation within 24 hours (see Fig. S3 in the supplementary material and data not shown). This and the fact that FRS2α was very low or absent in luminal epithelial cells of mature prostates, suggest that FRS2α is not essential to FGFR2 signaling with regard to its effects on the androgen-dependence of adult prostates.

The prostate is one of the few organs that have regenerative capacity in mice. Deprivation of androgen by orchiectomy and subsequent restoration induces rapid regression and regeneration, respectively. Although expression of FRS2α was very low or absent in the mature resting prostate epithelium, its expression was significantly increased in the regenerating epithelial cells induced by androgen. Although, overall, the androgen-induced regeneration of the prostate was not blocked by the absence of FRS2α, the rate and extent of proliferation during the process were compromised (Fig. 6). Thus, the elevated expression of FRS2α in regenerating epithelial cells contributes to the rate of androgen-induced prostate regeneration, but is not essential for it.

FRS2α-mediated signals in prostatic tumorigenesis

FRS2α has four tyrosine phosphorylation sites for GRB2 binding that link the FGFR kinase to the PI3 kinase/AKT pathway, and two for SHP2 (also known as PTPN11 – Mouse Genome Informatics) binding that link it to the MAP kinase pathway and are important for mediating mitogenic signals of FGFR (Gotoh et al., 2004; Kouhara et al., 1997; Ong et al., 1996; Ong et al., 1997; Xu and Goldfarb, 2001). The four GRB2-binding sites are required for mediating signals to activate the FiRE enhancer element of the mouse syndecan 1 gene (Zhang et al., 2007). We previously reported that FRS2α phosphorylation by FGFR kinases in rat prostate tumor cells is FGFR isotype-specific and associated with the promotion of cell proliferation by the presence of ectopic FGFR1 (Wang et al., 2002). Here we showed that from the early branching morphogenesis to mature stages, the expression of FRS2α in luminal epithelial cells of mouse prostates was proportional to the number of cells actively engaged in proliferation. Expression of FRS2α was transiently activated in the luminal epithelial cells during regeneration and appeared in PIN lesions and tumors where the cells were also actively proliferating. Our unpublished results using in situ hybridization have confirmed that that *Fgfr1* is not expressed in prostate epithelial cells during development, or during androgen-induced regeneration, or in resting mature prostates. Moreover, prostate epithelial cell-specific ablation of *Fgfr1* using $Nkx3.1^{Cre}$ induced no detectable abnormalities in prostate development or regeneration of mature prostates. However, FGRF1 was apparently expressed in the epithelial cells of lesion foci in the TRAMP prostate (Fig. 7A). Thus, the coincidence of the ectopic appearance of FGFR1 coupled with the constitutive expression of FRS2α might support and drive the neoplastic properties of the tumors, particularly with respect to mitogenesis. Prevention of expression of ectopic FGFR1 in tumor epithelial cells by a cross between ablation of the *Fgfr1* alleles specifically in prostate epithelial cells and the TRAMP mice should shed light on this subject. Together, the results reveal that the ectopic FGFR1/FRS2α signaling axis is a feature of the TRAMP tumor epithelial cells. Disruption of the axis by ablation of the $Frs2\alpha$ alleles is likely to interfere with tumor initiation and progression in the TRAMP model.

In summary, we report that FRS2α is spatiotemporally expressed in the prostatic epithelium and plays a role in prostate development, androgen-driven regeneration and tumorigenesis. The major role appears to be in mediation of prostatic epithelial cell proliferation in these three processes, rather than a direct effect on androgen responsiveness and differentiated function. The prostate epithelial cell-specific $Frs2\alpha^{cn}$ mice provide an additional useful model for scrutinizing not only the molecular mechanisms underlying prostate growth and development, but also how prostate cancer cells escape from strict controls on tissue homeostasis to propagate autonomously.

We thank Mary Cole for critical reading of the manuscript. The work was supported by AHA0655077Y from the America Heart Association, DAMD17-03-0014 (F.W.) from the US Department of Defense, and CA96824 (F.W.), CA115985 (M.M.S.), DK076602 (M.M.S.), CA59971 (W.L.M.) and CA84296 (N.M.G.) from the NIH.

Supplementary material

Supplementary material for this article is available at http://dev.biologists.org/cgi/content/full/135/4/????/DC1

References

Bhatia-Gaur, R., Donjacour, A. A., Sciavolino, P. J., Kim, M., Desai, N., Young, P., Norton, C. R., Gridley, T., Cardiff, R. D., Cunha, G. R. et al. (1999). Roles for Nkx3.1 in prostate development and cancer. *Genes Dev.* **13**, 966-977.

Donjacour, A. A. and Cunha, G. R. (1988). The effect of androgen deprivation on branching morphogenesis in the mouse prostate. *Dev. Biol.* **128**, 1-14.

Donjacour, A. A., Thomson, A. A. and Cunha, G. R. (2003). FGF-10 plays an essential role in the growth of the fetal prostate. *Dev. Biol.* **261**, 39-54.

Economides, K. D. and Capecchi, M. R. (2003). Hoxb13 is required for normal differentiation and secretory function of the ventral prostate. *Development* **130**, 2061-2069.

Foster, B. A., Gingrich, J. R., Kwon, E. D., Madias, C. and Greenberg, N. M. (1997). Characterization of prostatic epithelial cell lines derived from transgenic adenocarcinoma of the mouse prostate (TRAMP) model. *Cancer Res.* **57**, 3325-3330.

Foster, B. A., Kaplan, P. J. and Greenberg, N. M. (1999). Characterization of the FGF axis and identification of a novel FGFR1iiic isoform during prostate cancer progression in the TRAMP model. *Prostate Cancer Prostate Dis.* **2**, 76-82.

Giri, D., Ropiquet, F. and Ittmann, M. (1999). FGF9 is an autocrine and paracrine prostatic growth factor expressed by prostatic stromal cells. *J. Cell. Physiol.* **180**, 53-60.

Gotoh, N., Laks, S., Nakashima, M., Lax, I. and Schlessinger, J. (2004). FRS2 family docking proteins with overlapping roles in activation of MAP kinase have distinct spatial-temporal patterns of expression of their transcripts. *FEBS Lett.* **564**, 14-18.

Hadari, Y. R., Gotoh, N., Kouhara, H., Lax, I. and Schlessinger, J. (2001). Critical role for the docking-protein FRS2 alpha in FGF receptor-mediated signal transduction pathways. *Proc. Natl. Acad. Sci. USA* **98**, 8578-8583.

Huang, L., Pu, Y., Alam, S., Birch, L. and Prins, G. S. (2005). The role of Fgf10 signaling in branching morphogenesis and gene expression of the rat prostate gland: lobe-specific suppression by neonatal estrogens. *Dev. Biol.* **278**, 396-414.

Jin, C., McKeehan, K., Guo, W., Jauma, S., Ittmann, M. M., Foster, B., Greenberg, N. M., McKeehan, W. L. and Wang, F. (2003a). Cooperation between ectopic FGFR1 and depression of FGFR2 in induction of prostatic intraepithelial neoplasia in the mouse prostate. *Cancer Res.* **63**, 8784-8790.
Jin, C., McKeehan, K. and Wang, F. (2003b). Transgenic mouse with high Cre recombinase activity in all prostate lobes, seminal vesicle, and ductus deferens. *Prostate* **57**, 160-164.
Kaplan-Lefko, P. J., Chen, T. M., Ittmann, M. M., Barrios, R. J., Ayala, G. E., Huss, W. J., Maddison, L. A., Foster, B. A. and Greenberg, N. M. (2003). Pathobiology of autochthonous prostate cancer in a pre-clinical transgenic mouse model. *Prostate* **55**, 219-237.
Kouhara, H., Hadari, Y. R., Spivak-Kroizman, T., Schilling, J., Bar-Sagi, D., Lax, I. and Schlessinger, J. (1997). A lipid-anchored Grb2-binding protein that links FGF-receptor activation to the Ras/MAPK signaling pathway. *Cell* **89**, 693-702.
Kwabi-Addo, B., Ropiquet, F., Giri, D. and Ittmann, M. (2001). Alternative splicing of fibroblast growth factor receptors in human prostate cancer. *Prostate* **46**, 163-172.
Lamm, M. L., Podlasek, C. A., Barnett, D. H., Lee, J., Clemens, J. Q., Hebner, C. M. and Bushman, W. (2001). Mesenchymal factor bone morphogenetic protein 4 restricts ductal budding and branching morphogenesis in the developing prostate. *Dev. Biol.* **232**, 301-314.
Lin, H. Y., Xu, J., Ischenko, I., Ornitz, D. M., Halegoua, S. and Hayman, M. J. (1998). Identification of the cytoplasmic regions of fibroblast growth factor (FGF) receptor 1 which play important roles in induction of neurite outgrowth in PC12 cells by FGF-1. *Mol. Cell. Biol.* **18**, 3762-3770.
Lin, Y., Liu, G., Zhang, Y., Hu, Y. P., Yu, K., Lin, C., McKeehan, K., Xuan, J. W., Ornitz, D. M., Shen, M. M. et al. (2007a). Fibroblast growth factor receptor 2 tyrosine kinase is required for prostatic morphogenesis and the acquisition of strict androgen dependency for adult tissue homeostasis. *Development* **134**, 723-734.
Lin, Y., Zhang, J., Zhang, Y. and Wang, F. (2007b). Generation of an Frs2alpha conditional null allele. *Genesis* **45**, 554-559.
Liu, W., Selever, J., Murali, D., Sun, X., Brugger, S. M., Ma, L., Schwartz, R. J., Maxson, R., Furuta, Y. and Martin, J. F. (2005). Threshold-specific requirements for Bmp4 in mandibular development. *Dev. Biol.* **283**, 282-293.
Lu, W., Luo, Y., Kan, M. and McKeehan, W. L. (1999). Fibroblast growth factor-10. A second candidate stromal to epithelial cell andromedin in prostate. *J. Biol. Chem.* **274**, 12827-12834.
McDougall, K., Kubu, C., Verdi, J. M. and Meakin, S. O. (2001). Developmental expression patterns of the signaling adapters FRS-2 and FRS-3 during early embryogenesis. *Mech. Dev.* **103**, 145-148.
McKeehan, W. L., Wang, F. and Kan, M. (1998). The heparan sulfate-fibroblast growth factor family: diversity of structure and function. *Prog. Nucleic Acid Res. Mol. Biol.* **59**, 135-176.
Ong, S. H., Goh, K. C., Lim, Y. P., Low, B. C., Klint, P., Claesson-Welsh, L., Cao, X., Tan, Y. H. and Guy, G. R. (1996). Suc1-associated neurotrophic factor target (SNT) protein is a major FGF-stimulated tyrosine phosphorylated 90-kDa protein which binds to the SH2 domain of GRB2. *Biochem. Biophys. Res. Commun.* **225**, 1021-1026.
Ong, S. H., Lim, Y. P., Low, B. C. and Guy, G. R. (1997). SHP2 associates directly with tyrosine phosphorylated p90 (SNT) protein in FGF-stimulated cells. *Biochem. Biophys. Res. Commun.* **238**, 261-266.
Ong, S. H., Guy, G. R., Hadari, Y. R., Laks, S., Gotoh, N., Schlessinger, J. and Lax, I. (2000). FRS2 proteins recruit intracellular signaling pathways by binding to diverse targets on fibroblast growth factor and nerve growth factor receptors. *Mol. Cell. Biol.* **20**, 979-989.
Park, J. H., Walls, J. E., Galvez, J. J., Kim, M., Abate-Shen, C., Shen, M. M. and Cardiff, R. D. (2002). Prostatic intraepithelial neoplasia in genetically engineered mice. *Am. J. Pathol.* **161**, 727-735.
Podlasek, C. A., Duboule, D. and Bushman, W. (1997). Male accessory sex organ morphogenesis is altered by loss of function of Hoxd-13. *Dev. Dyn.* **208**, 454-465.
Polnaszek, N., Kwabi-Addo, B., Wang, J. and Ittmann, M. (2004). FGF17 is an autocrine prostatic epithelial growth factor and is upregulated in benign prostatic hyperplasia. *Prostate* **60**, 18-24.
Powers, C. J., McLeskey, S. W. and Wellstein, A. (2000). Fibroblast growth factors, their receptors and signaling. *Endocr. Relat. Cancer* **7**, 165-197.
Pu, Y., Huang, L., Birch, L. and Prins, G. S. (2007). Androgen regulation of prostate morphoregulatory gene expression: Fgf10-dependent and -independent pathways. *Endocrinology* **148**, 1697-1706.
Rabin, S. J., Cleghon, V. and Kaplan, D. R. (1993). SNT, a differentiation-specific target of neurotrophic factor-induced tyrosine kinase activity in neurons and PC12 cells. *Mol. Cell. Biol.* **13**, 2203-2213.
Ropiquet, F., Giri, D., Lamb, D. J. and Ittmann, M. (1999). FGF7 and FGF2 are increased in benign prostatic hyperplasia and are associated with increased proliferation. *J. Urol.* **162**, 595-599.
Soriano, P. (1999). Generalized lacZ expression with the ROSA26 Cre reporter strain. *Nat. Genet.* **21**, 70-71.
Sugimura, Y., Cunha, G. R. and Donjacour, A. A. (1986). Morphogenesis of ductal networks in the mouse prostate. *Biol. Reprod.* **34**, 961-971.
Thomson, A. A. and Cunha, G. R. (1999). Prostatic growth and development are regulated by FGF10. *Development* **126**, 3693-3701.
Wang, F. and McKeehan, W. L. (2003). The fibroblast growth factor (FGF) signaling complex. In *Handbook of Cell Signaling*. Vol. 1 (ed. R. Bradshaw and E. Dennis), pp. 265-270. New York: Academic/Elsevier Press.
Wang, F., McKeehan, K., Yu, C. and McKeehan, W. L. (2002). Fibroblast growth factor receptor 1 phosphotyrosine 766, molecular target for prevention of progression of prostate tumors to malignancy. *Cancer Res.* **62**, 1898-1903.
Xu, H. and Goldfarb, M. (2001). Multiple effector domains within SNT1 coordinate ERK activation and neuronal differentiation of PC12 cells. *J. Biol. Chem.* **276**, 13049-13056.
Zhang, Y., McKeehan, K., Lin, Y., Zhang, J. and Wang, F. (2007). FGFR1 tyrosine phosphorylation regulates binding of FRS2alpha but not FRS2beta to the receptor. *Mol. Endocrinol*. doi: 10.1210/me.2007-0140.